

PERFORMANCE ASSESSMENT OF STEEL TRUSS RAILWAY BRIDGE WITH CURVED TRACK

MICHAL VENGLÁR*, KATARÍNA LAMPEROVÁ, MILAN SOKOL

Slovak University of Technology, Faculty of Civil Engineering, Department of Structural Mechanics, Radlinského 11, 810 05 Bratislava, Slovakia

* corresponding author: michal.venglar@stuba.sk

ABSTRACT. Non-destructive Structural Health Monitoring techniques can be incorporated into bridge integrity management by assessing structural conditions. This paper describes a performance assessment of a steel truss railway bridge in Bratislava using vibration-based techniques as a further part of maintenance in addition to standard visual inspections. To obtain the necessary data, a multipurpose measuring system was used. Various types of data were measured, e.g. accelerations, strains, and displacements. The advantage of the multipurpose measuring system was that the traffic over the bridge was not restricted, even though the bridge carries only a single curved track. Two test campaigns were conducted to assess the performance of the bridge. One campaign was devoted to measuring ambient vibrations in order to perform the operational modal analysis, and the second was carried out to measure strains and displacements during a train passage. The results show a successful system identification of the structure using ambient vibrations; and a finite element model was verified and validated by a comparison of strains and displacements, as well as by modal parameters. According to the results obtained, the structural health of the investigated bridge was satisfactory.

KEYWORDS: System identification, performance assessment, steel truss bridge, ambient vibration, train passage, FEM model, curved track.

1. INTRODUCTION

Bridges represent critical components of transportation networks, whether road or railway. Therefore, administrators of railway networks around the world are the most responsible for ensuring the integrity of the networks with railway bridges being an integral part of these networks. In many countries, only visual inspections are periodically carried out on bridges to detect structural deviations. To illustrate on the example of Slovakia: The Railways of the Slovak Republic (ŽSR) have their own rules of bridge inspection and the standard visual inspection of every bridge is carried out by the employees of ŽSR once every three years, unless the bridge is in poor condition (according to the rating index). Maintenance activities can be prioritised accordingly. However, the results of visual inspections depend on the skill of the inspectors and can be strongly affected by human errors and, therefore, sometimes not be reliable. In addition to that, they are time-consuming [1]. However, an interesting project “Methods for achieving sustainability of industrial heritage steel bridges” with ID: DG18P02OVV033 is being solved in the Czech Republic to check and verify the state of steel bridges, as well as to ensure integrity of the important parts of networks. The book [2] shows some results of that project. Main failures are also summarised there, e.g. fatigue cracks, corrosion (loss of material), extreme deflections caused by various accidents, malfunction of supports, or simple degradation during operation. As a result of this state, additional testing techniques,

such as structural health monitoring (SHM) [3, 4] are required. According to [5], SHM could be combined with and supplement visual inspections, which, however, cannot be omitted. According to [6], the information obtained by SHM should also be used in decision-making of administrators, and interdisciplinary cooperation is necessary. At the same time, information must be based on thoughtful measurements and analyses, and not on subjective estimates. Besides that, the costs of experimental tests are negligible as compared to bridge renovation costs [7].

In recent years, various approaches to SHM have been established, for example, classical SHM (described in the following paragraph) or inverse SHM approach (with moving sensors) used mainly on railway bridges [8–10]. However, researchers also study the possibility of using low-cost sensors as stationary real-time systems [11]. In the research field of vibration-based SHM methods [12–19], the system identification is mentioned as the first step [20] to determine the current health of the structure [21]. The task involves the identification of a dynamic system, which is described by specific stiffness, damping, and mass parameters [22, 23]. After that, various damage detection and localisation algorithms can be used [24].

Therefore, in this paper, the initial system identification of the observed steel truss railway bridge (Figure 1) is described and the first results are stated to represent a background for future measurements and decision-making by the administrators. The paper also details the preparation and the performance



FIGURE 1. Steel truss railway bridge in Bratislava.

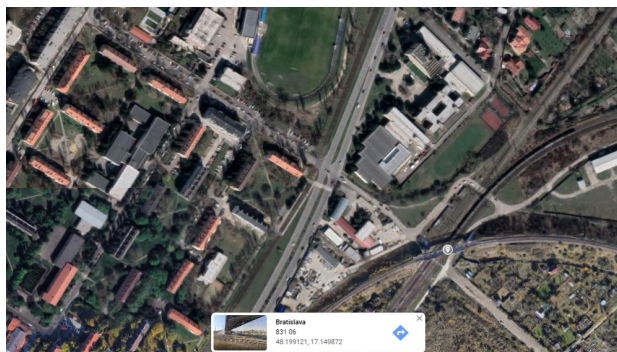


FIGURE 2. Location of the steel truss railway bridge in Bratislava, from [25].

of dynamic tests (together with the quasi-static one) carried out during the first phase of the investigation. In this case, the fact that the track on the bridge is curved also posed a problem. As a result of this curvature, the overall stress distribution, especially on the bridge deck elements, but also on the main girders, depends not only on the weight of a particular train but also on its speed and the corresponding horizontal centrifugal force.

The paper consists of several sections: Section 2 describes the bridge; Section 3 deals with the preparation of experimental measurements, e.g. the characterisation of the FEM model and the placement of sensors; Section 4 is devoted to the analyses of measured accelerations; the strains are compared with numerical calculations; Section 5 discusses the results. Finally, the main conclusions are presented in Section 6.

2. BRIDGE DESCRIPTION

The steel bridge is located at kilometer 6.124 of the main connection between Bratislava and Žilina and crosses over the four tracks of the line no. 120 (see Figure 2). The track connects the stations Bratislava – Vineyards and Bratislava – East on the line no. 609. The load-bearing structure of the single span-bridge (the total span is 56 m) consists of two main truss girders with a lower open bridge deck. The bridge deck consists of floor beams (with a length of 6.3 m) and stringers (with a length of 5.6 m). The structure has pinned supports on the side of the Bratislava – East station (Figure 1, on the left side and Figure 3, on the right side) and rollers towards the Bratislava – Vineyards station.

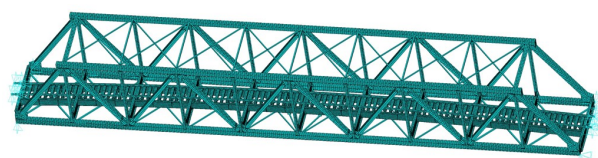


FIGURE 3. Initial FEM model with curved track.

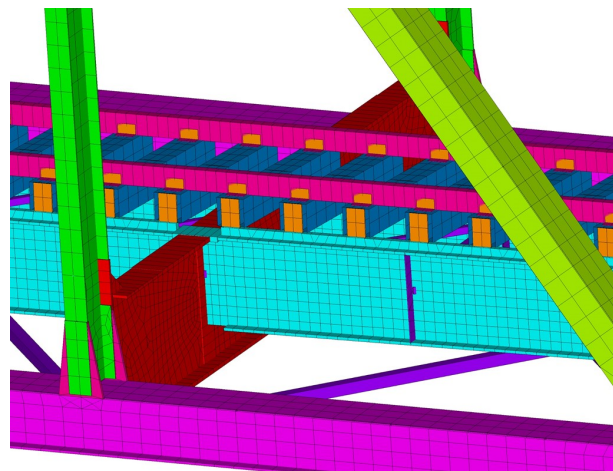


FIGURE 4. Detail of the FEM model with curved track.

The substructure consists of reinforced concrete supports with sloping wing walls. The bridge carries a single-track railway (Figure 3) (which is curved with a radius of 400 m and is also elevated) with a speed limit of 80 km h^{-1} .

3. PREPARATION AND EXECUTION OF TESTS

Dynamic tests were performed twice in a one-month period. According to [26], the sensor configuration is the key factor of the entire testing process. Therefore, the bridge was equipped with various sensors, for example, accelerometers, strain gauges, and thermocouples. IBIS-S interferometric radar was also used to measure bridge displacements. These sensors and devices were used to form a multipurpose measuring system [27]. The measurements were preceded by a review of available project documentation and preparation of the initial finite element method (FEM) model. The initial modal analysis was performed using this FEM model to determine the optimal placement of the accelerometers. A quasi-static analysis was also carried out numerically to obtain expected stresses on the stringers, where strain gauges were installed as half-bridge completions.

3.1. FEM MODEL

The detailed numerical model (Figure 3) of the bridge was prepared. A special attention was paid to modelling the surface bridge deck, which was guided along a curve. To monitor stresses in detail in any place, the load-bearing components (lower and upper chords, diagonal members, floor beams, stringers, and bracings)

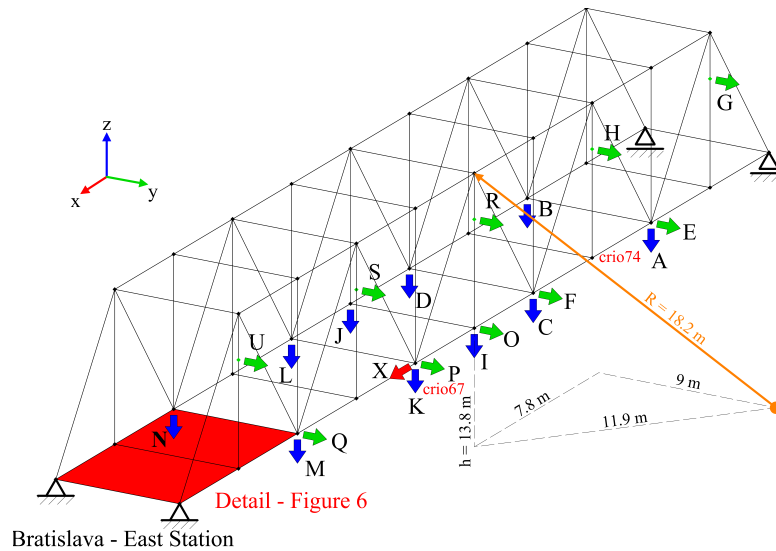


FIGURE 5. Locations of accelerometers and IBIS-S radar along the bridge.

were mostly modelled as shell elements of appropriate dimensions (according to the documentation). In addition, rails and sleepers were also modelled for a proper load distribution (Figure 4).

The materials used are described in the following Table 1.

Material	E [GPa]	Poisson's ratio [-]	Density [kg m ³]
Steel	210	0.30	7850
Wood	13	0.40	800

TABLE 1. Characteristics of the materials used.

The weight of the entire structure, including rails, sleepers, and other non-bearing parts of the structure such as sidewalks and railings, is approximately 240 tons. The non-bearing structure parts were modelled as added mass.

3.2. SENSOR NETWORK

The chosen positions of the accelerometers (Figure 5) were determined from the initial modal analysis performed on the FEM model described above.

The acceleration was measured in the vertical directions (in the direction of Z axis) by ten sensors to identify the vertical bending and torsional mode-shapes. In addition, ten other sensors were positioned in the horizontal direction. These were used to analyse horizontal (in the direction of the Y axis) and torsional mode-shapes. The last two sensors were used to determine whether the sliding supports work properly. In order to eliminate future environmental effects on modal parameters, temperature sensors were placed in proximity of the chosen accelerometers. Six contact thermocouples were positioned evenly along the bridge. The other two sensors measured air temperature. Furthermore, several strain gauges (Figure 6)

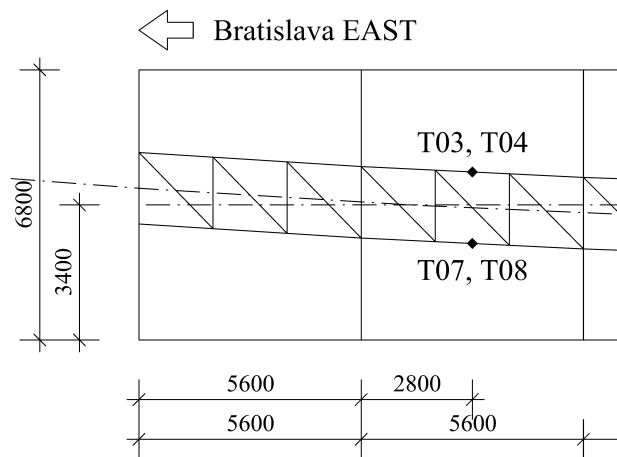


FIGURE 6. Locations of strain gauges on the bridge.

were attached to the second stringers from the side of the fixed supports (the station Bratislava – East).

3.3. INTERFEROMETRIC RADAR IBIS-S

The IBIS-S interferometric radar represents a device suitable for measuring displacements of several points along the structure. The radar transmits microwave frequencies in short pulses and, based on the time difference between the transmitted and received signals, the displacements of multiple points of the structure are determined [28]. Depending on the intensity of the reflected signal, a measurement accuracy of 0.1 mm can be easily achieved. The use of radar interferometry is, therefore, highly suitable for measuring the response of bridges without traffic restrictions.

Although it is possible to measure at several locations at the same time, in this case, for the sake of simplicity, attention was paid to measuring displacements in one location only. The interferometric radar was oriented toward the upper joint of the main truss girder. The exact measured point (Figure 7) is located



FIGURE 7. Exact point of the bridge structure monitored by IBIS-S radar.

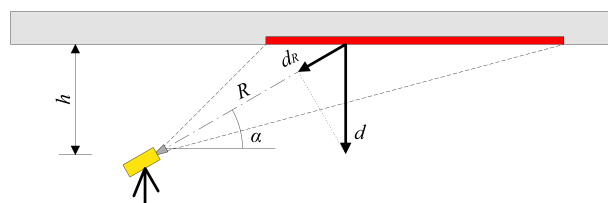


FIGURE 8. Projection of the measured displacement d_R .

on the main girder of the bridge, in the middle of the span.

The radar measures displacements (changes in distance) in the radial direction d_R (Figure 8). The radial displacement d_R can be projected into the direction of the effective displacement d (in this case in the vertical direction) according to (1).

$$d = \frac{d_R}{\sin \alpha} = d_R \frac{R}{h} \quad (1)$$

The position of the radar is marked with an orange dot in Figure 5. The orange arrow shows the radial distance R between the measured point and the radar. In this case, R was approximately 18.2 m.

3.4. PERFORMANCE OF THE DYNAMIC TESTS

As mentioned above, measurements were performed over two days, one month apart. The temperature reached 5 °C at the time of the first observation and 10 °C on the second day of the test.

One campaign was devoted to measuring ambient vibrations in order to perform the operational modal analysis, and the second to measuring strains and displacements during train passages. In the course of the measurements, the IBIS-S radar was located near the abutment with fixed supports (Figure 5).

The displacement measurements were performed in a dynamic mode with a sampling frequency of 200 Hz and a resolution of the measured points equal to 0.75 m.

The traffic on the bridge is usually not very heavy; therefore, many records of ambient vibrations were

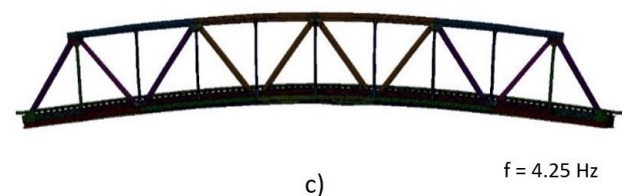
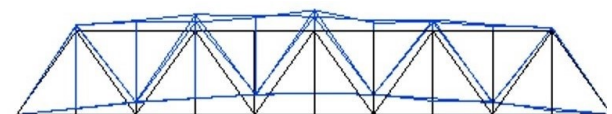
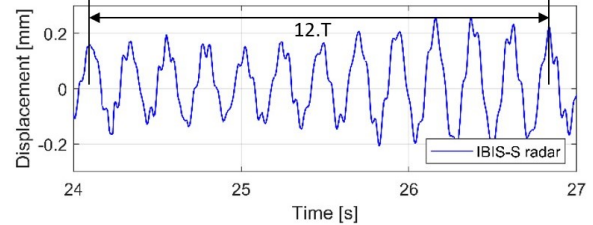
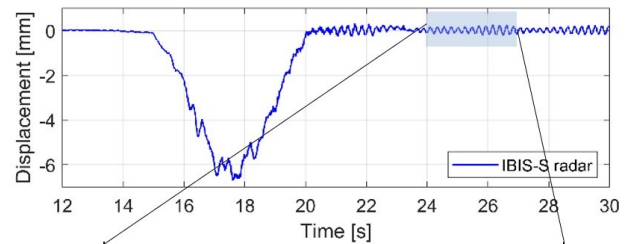


FIGURE 9. The second identified natural frequency a) vertical displacements caused by the train passage b) mode-shape from the measured accelerations, and c) mode-shape obtained by the FEM model.

logged using the multichannel data acquisition (DAQ) system. Hence, dynamic properties could be extracted from the ambient data. Additionally, the passages of locomotives and cargo trains were recorded during the second campaign. The stiffness parameter of the FEM model was verified by a quasi-static test of the passing train. The behaviour of the bridge deck, mainly of the most loaded stringers, was compared to the calculated stresses.

4. BRIDGE PERFORMANCE ASSESSMENT

4.1. ANALYSES OF MEASURED DATA

Ambient vibration data were prepared using the codes for pre-processing and processing (using stochastic subspace identification – SSI), as mentioned in [29]. The data were then used similarly in the ModalVIEW software as in [30]. The discrete-time Fourier transform (DTFT; described in [31]) was used to identify natural frequencies from the measured displacements in order to compare them to those identified from the measured accelerations.

As can be seen in Figure 9 a), the displacements were extracted after the train (the single locomotive

Mode-shape no.	Description	Calculated freq. [Hz]	Measured freq. [Hz]	Cross-MAC [-]
1	in Y direction	2.48	2.56	0.99
2	in Z direction	4.25	4.33	0.99
3	in Y direction	4.50	4.78	0.98
4	in Y direction	6.16	6.48	0.99
5	around X axis	7.11	7.42	1.00
6	in Y direction	8.33	8.85	0.96
7	in X direction	9.39	–	–
8	in Z direction	11.31	11.09	0.95
9	in Y direction	11.37	11.91	0.92

TABLE 2. Comparison of identified mode-shapes and corresponding natural frequencies, as well as Cross-MAC values.

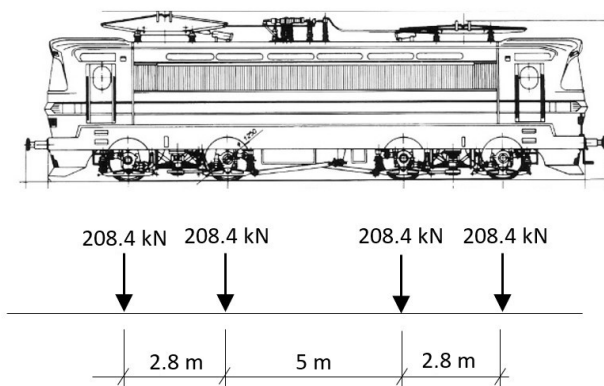


FIGURE 10. Locomotive type 240 with axle loadings and spacings.

240 – Figure 10) left the bridge, that is, between 24–27 s. The train speed during this passage (in the first campaign) was approximately 40 km/h. This is also described in Section 4.3 in more detail.

4.2. SYSTEM IDENTIFICATION

Natural frequencies and damping were identified using the SSI method. It can be seen in Table 2 that the calculated and obtained natural frequencies are in good agreement. Furthermore, Cross-MAC values were calculated similarly as in [32], and the values obtained ensured that a model update of the initial FEM was unnecessary. This can prove that the bearing structure has not shown any critical damage (malfunction of the supports or extreme deflections of members) since it was opened in 1976. Moreover, the real structure shows slightly greater parameters of stiffness. Identified damping ratios (Table 3) are valuable information for a future part of the study, when the remaining fatigue life will be calculated.

4.3. QUASI-STATIC TEST

The above-mentioned fact that the stiffness was slightly greater was also confirmed by the measurement of displacement. For example, the measured

Mode-shape no.	Description	Identified damping [%]
1	in Y direction	1.32
2	in Z direction	2.34
3	in Y direction	0.76
4	in Y direction	1.43
5	around X axis	1.39
6	in Y direction	0.85

TABLE 3. Identified damping ratios for individual mode-shapes.

displacement during train passages (quasi-static part of the displacement in the middle of the bridge, on the side of the outer curve of the railway) reached approximately 6.3 mm representing approximately 95 % of the quasi-static displacement calculated using influence lines.

The eccentricity of the vertical load (uneven distribution of the vertical load on the individual rails) must also be taken into consideration in the calculations due to the centrifugal force Q_h , which arises because the railway track is curved. The eccentricity of the vertical load e was calculated according to the geometry in Figure 11:

$$e = \frac{u}{s} h_C, \quad (2)$$

where h_C is the value of the centrifugal forces above the top plane of the rails and u is the value of the height difference between two rails. According to [33], the height h_C is 1.8 m. The parameter s is the track gauge and, in most cases in Slovakia, has a value equal to 1.435 m. The magnitude of the centrifugal forces depends on the speed of the train [33] and is given as:

$$Q_H = \frac{Mv^2}{r}, \quad (3)$$

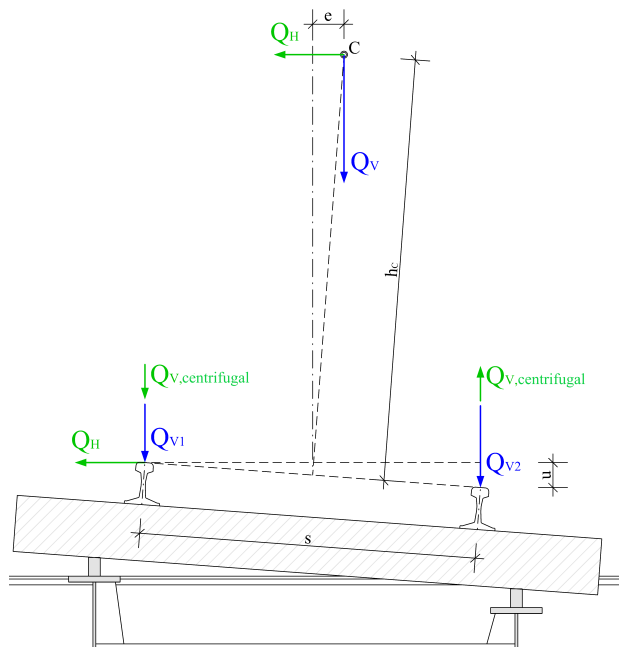


FIGURE 11. Scheme of quasi-static axle forces.

where M is the mass per axle, v is the speed of the passing train, and r is the radius of the track curve. Vertical forces $Q_{V,centrifugal}$ were calculated according to:

$$Q_{V,centrifugal} = \frac{Q_H h_c}{s}. \quad (4)$$

The redistribution of the total vertical axle force Q_V was determined according to the following equation:

$$Q_{V1} = \frac{Q_V(\frac{s}{2} - e)}{s} \quad (5)$$

$$Q_{V2} = \frac{Q_V(\frac{s}{2} + e)}{s}, \quad (6)$$

where Q_{V1} is the vertical axle force for the inner curve of the track (rail with a smaller radius), and Q_{V2} is the vertical axle force for the outer curve. Due to the geometry of the track (Figure 11), the rail in the inner curve would be subjected to a load higher by 46% higher under static action or at extremely low speeds [33]. However, the size of the load on individual rails is significantly affected by the value of centrifugal forces. The load on the rail on the outer curve increases with increasing speed. Unlike bridges with straight rails, the expected response of the structure may be different on the side closer to the outer curve and on the side closer to the inner curve. The railway locomotive – type no. 240 is 16 m long, and Figure 10 shows the axle load and axle spacing of the locomotive used for the quasi-static test. The total weight is 85 tons.

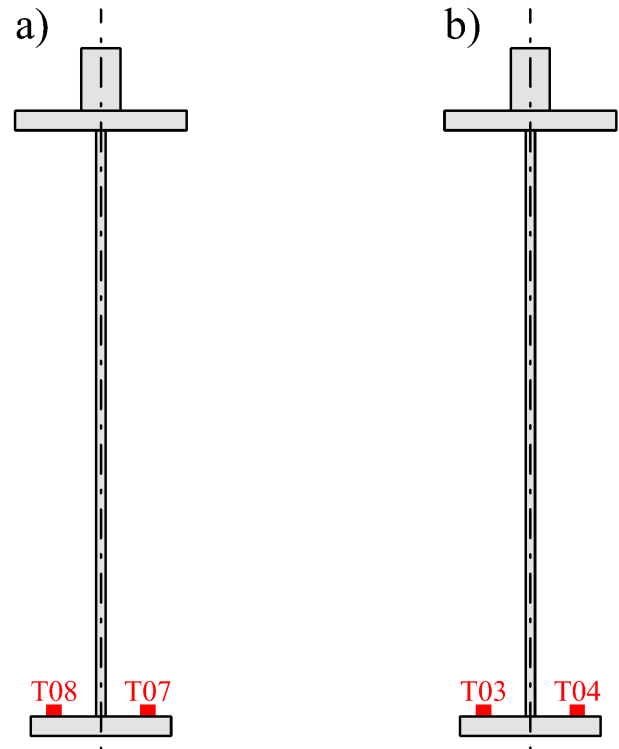


FIGURE 12. Strain gauges (T03, T04, T07 and T08) attached to the second stringers a) outer b) inner.

4.4. COMPARISON OF THE STRAIN ON THE STRINGERS

The same locomotive was used to calculate the strain on the stringers. The influence lines calculated by the numerical model were utilised to perform the quasi-static analysis. It can be seen in Figure 12 that the strain gauges were installed on the bottom flange of the second stringers in the middle of the span.

Figs. 13 and 14 show the comparison between calculated and measured stresses during the train passage. The outer stringer (Figure 13) shows a better agreement between the calculation and the measurement. As a result, there is no evidence that the investigated part of the bridge deck is damaged (e.g., by corrosion). In the case of the inner stringer (Figure 14), the difference is up to 25%. It can be seen that the measured stresses are smaller than the calculated ones. This is due to the fact that some non-structural parts (rails, sleepers) also carry a part of the load and it is likely that the thickness of the steel elements is slightly greater than assumed in the analysis – the geometry in FEM analysis was taken from the design values. Other possible reasons should be investigated in more detail in the future. We generally consider the agreement between the measured and calculated stresses to be very good. The difference in the accuracy of the agreement of the results between Figs. 13 and 14 may be caused by an inaccurate determination of the train speed, which influences the distribution of the load between the outer and inner stringer. This can be seen in small differences when the minimum

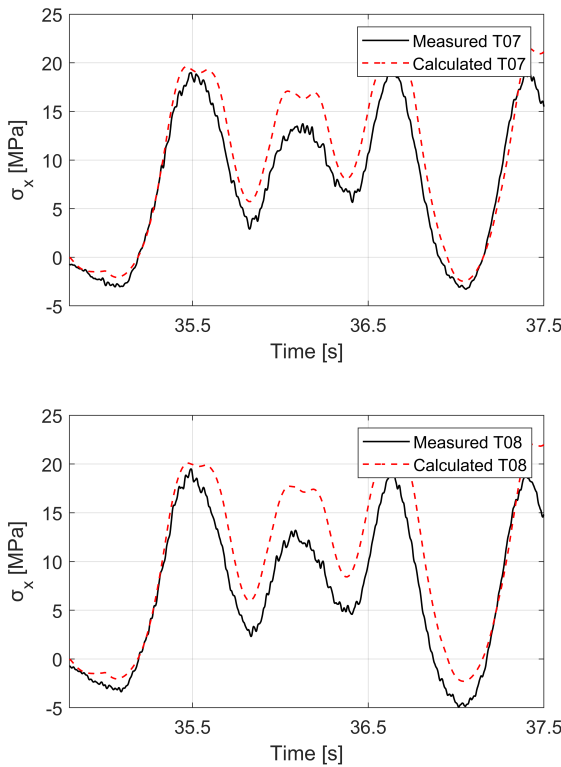


FIGURE 13. Comparison of normal stresses on the outer stringer – strain gauges: T07 (top) and T08 (bottom).

values occur. At a time of about 35.25 s, there is a good agreement, and at a time of 36.75 s, the measured minimum of stresses occurs a little earlier. This result points to the importance of considering multiple details in structural health monitoring.

4.5. COMPARISON OF DISPLACEMENTS

Figure 15 shows a comparison of the measured and calculated displacements of the monitored point of the structure (Figure 7). In this case, the resulting values arise due to the passage of a train consisting of only two connected locomotives (both no. 240, Figure 10). During the second measuring campaign, the locomotives moved at a speed of approximately 4.6 km/h. Due to the fact that the bridge was not closed, the trains' speeds were random. However, the slow passage was very useful, allowing a comparison of the measured data with the quasi-static analysis. The difference between the test and analysis values is only 4 %, which is a very satisfactory result. Because the speed and geometry of the track is known, it is possible to estimate the displacement on the opposite side of the bridge cross-section. This consideration concerns only the estimation of the maximum displacement on the bridge. In this case, the value at this point should be 11 % higher than at the measured point (Figure 16).

This value could be verified, e.g. by synchronized measurement with two radars on both sides of the structure or by a radar on one side and another mea-

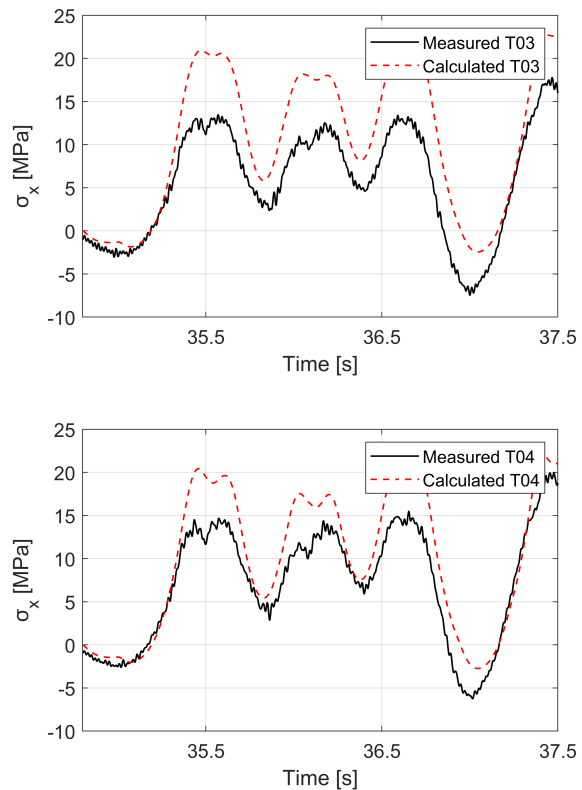


FIGURE 14. Comparison of normal stresses on the inner stringer – strain gauges: T03 (top) and T04 (bottom).

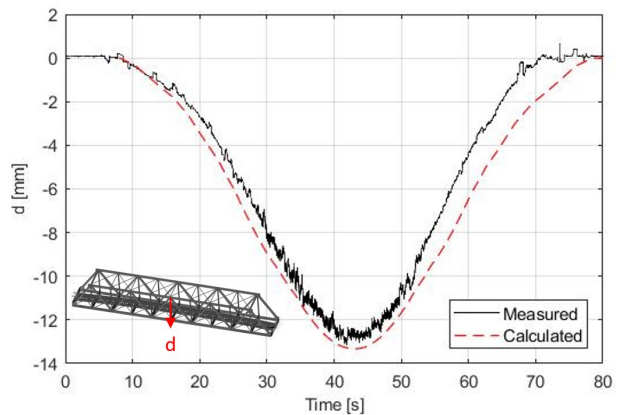


FIGURE 15. Comparison of measured and calculated displacement.

suring device on the other side of the bridge. These results show that we can relatively accurately determine the deflections of any load that occur during the measurement on the bridge using this method of measurement and a subsequent analysis. The results show that an agreement between the measured and calculated values can be achieved up to a level of $\pm 5\%$. The presented results proved the above-mentioned results from the operational modal analysis. Any larger difference between the measured and calculated values can lead to the acquisition of important data on the incorrect response of the bridge, and, consequently,

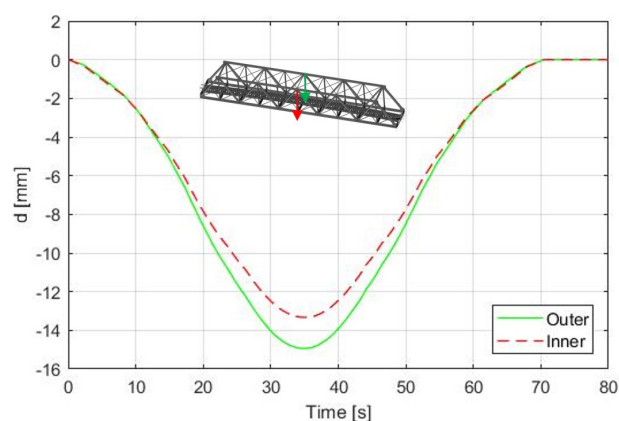


FIGURE 16. Comparison of maximum displacements on both sides of the cross-section.

such a result can serve as an impulse for the responsible authorities that something is wrong with the bridge and it needs due attention.

5. DISCUSSION

The results obtained confirm that the system identification was successful thanks to the satisfactory measurements performed as well as an accurate FEM model. Damping ratios represent highly valuable information. The remaining fatigue life can be evaluated in the future using the values obtained. It is necessary to state that the FEM model was prepared in more detail (rails were also modelled), and the documentation was, fortunately, sufficient. Due to this, the results of the initial FEM model were comparable to those of the measurements. The results can also be used to estimate possible deviations of the variance between the measurement results and numerical analysis, which, in our case, reaches 5% for displacements and about 15–25% for stresses. The possible reasons of differences in strains should be investigated in more detail in the future. It is also highly valuable that a good agreement of the results was achieved, even though it was a complicated case where the track is led over a bridge in a curve. As previously mentioned, measurements with radars on both sides of the structure can be carried out in the future to verify uneven displacements also experimentally. IBIS-S radars have the possibility to synchronize two or more radars.

6. CONCLUSIONS

In this study, a performance assessment of a curved track steel rail bridge was performed. In order to do that, a FEM model had to be created. Then, all measurements were performed without interruptions to the traffic over and under the bridge. This fact can prove to be an added value (performed in the presented way) for administrators of the infrastructure, as it allows for obtaining complementary information (in addition to the visual inspection) about

the structure without any disruptions. The data acquired and analysed show that it is not necessary to update the FEM model. All comparisons show an exact agreement between the real behaviour and the state modelled according to the available documentation and visual inspections. Because of that, the verified and validated FEM model can be used for a prediction analysis in the future. Consequently, it can be stated that there is no indication of any serious damage to the investigated structure after almost 50 years of operation (at the time of the tests). These results can also be used as a comparative base for future repetitions and as an additional information for the decision makers at ŽSR.

ACKNOWLEDGEMENTS

The authors gratefully acknowledge the contribution of the Scientific Grant Agency of the Slovak Republic under the grant VEGA no. 1/0230/22.

REFERENCES

- [1] S. C. Siriwardane. Vibration measurement-based simple technique for damage detection of truss bridges: A case study. *Case Studies in Engineering Failure Analysis* 4:50–58, 2015. <https://doi.org/10.1016/j.csefa.2015.08.001>.
- [2] P. Ryjáček, T. Rotter, V. Stančík, et al. *Metody pro zajištění udržitelnosti ocelových mostních konstrukcí industriálního kulturního dědictví [Methods for Achieving Sustainability of Industrial Heritage Steel Bridges]*. First printing. Czech Technical University in Prague, Prague, 2022. ISBN 978-80-01-06990-5.
- [3] C. Comisu, N. Taranu, G. Boaca, M. Scutaru. Structural health monitoring system of bridges. *Procedia Engineering* 199:2054–2059, 2017. <https://doi.org/10.1016/j.proeng.2017.09.472>.
- [4] H. Ceylan, K. Gopalakrishnan, S. Kim, et al. Highway infrastructure health monitoring using micro-electromechanical sensors and systems (MEMS). *Journal of Civil Engineering & Management* 19(1):188–201, 2014. <https://doi.org/10.3846/13923730.2013.801894>.
- [5] P. Haardt, R. Holst. Monitoring during life cycle of bridges to establish performance indicators. In *The Value of Structural Health Monitoring for the reliable Bridge Management*, p. 1–9. 2017. <https://doi.org/10.5592/CO/BSHM2017.4.2>.
- [6] M. Limongelli. SHM for informed management of civil structures and infrastructure. *Journal of Civil Structural Health Monitoring* 10(5):739–741, 2020. <https://doi.org/10.1007/s13349-020-00439-8>.
- [7] T. Plachý, M. Polák, P. Ryjáček. Assessment of an old steel railway bridge using dynamic tests. *Procedia Engineering* 199:3053–3058, 2017. <https://doi.org/10.1016/j.proeng.2017.09.555>.
- [8] A. Malekjafarian, E. O'Brien, P. Quirke, C. Bowe. Railway track monitoring using train measurements: An experimental case study. *Applied Sciences* 9(22):4859, 2019. <https://doi.org/10.3390/app9224859>.

- [9] S. Lorenzen, H. Berthold, M. Rupp, et al. *Bridge Safety, Maintenance, Management, Life-Cycle, Resilience and Sustainability*, chap. Deep learning based indirect monitoring to identify bridge natural frequencies using sensors on a passing train, pp. 401–409. CRC Press, 2022. <https://doi.org/10.1201/9781003322641-46>.
- [10] S. Urushadze, J. Yau, Y. Yang, J. Bayer. Theoretical and experimental verifications of bridge frequency using indirect method. In *Conference Proceedings of the Society for Experimental Mechanics Series*, pp. 153–158. 2020. https://doi.org/10.1007/978-3-030-12115-0_20.
- [11] S. Quqa, L. Landi, P. P. Diotallevi. Real time damage detection through single low-cost smart sensor. In *Eccomas Proceedia COMPDYN*, pp. 3914–3925. 2019. <https://doi.org/10.7712/120119.7196.19614>.
- [12] P. F. Giordano, M. P. Limongelli. Response-based time-invariant methods for damage localization on a concrete bridge. *Structural Concrete* **21**(4):1254–1271, 2020. <https://doi.org/10.1002/suco.202000013>.
- [13] K. Gkoktsi, A. Giaralis, R. P. Klis, et al. Output-only vibration-based monitoring of civil infrastructure via sub-nyquist/compressive measurements supporting reduced wireless data transmission. *Frontiers in Built Environment* **5**:111, 2019. <https://doi.org/10.3389/fbuil.2019.00111>.
- [14] E. Giordano, N. Mendes, M. G. Masciotta, et al. Expeditious damage index for arched structures based on dynamic identification testing. *Construction and Building Materials* **265**:120236, 2020. <https://doi.org/10.1016/j.conbuildmat.2020.120236>.
- [15] S. Quqa, L. Landi, P. P. Diotallevi. Instantaneous modal identification under varying structural characteristics: A decentralized algorithm. *Mechanical Systems and Signal Processing* **142**:106750, 2020. <https://doi.org/10.1016/j.ymsp.2020.106750>.
- [16] R. P. Finotti, A. L. Bonifácio, F. S. Barbosa, A. A. Cury. Evaluation of computational intelligence methods using statistical analysis to detect structural damage. *Mecánica Computacional* **34**(22):1389–1397, 2016.
- [17] M. Sysyn, U. Gerber, O. Nabochenko, et al. Indicators for common crossing structural health monitoring with track-side inertial measurements. *Acta Polytechnica* **59**(2):170–181, 2019. <https://doi.org/10.14311/AP.2019.59.0170>.
- [18] M. Sysyn, O. Nabochenko, U. Gerber, et al. Common crossing condition monitoring with on board inertial measurements. *Acta Polytechnica* **59**(4):423–434, 2019. <https://doi.org/10.14311/AP.2019.59.0423>.
- [19] M. Sysyn, O. Nabochenko, F. Kluge, et al. Common crossing structural health analysis with track-side monitoring. *Communications – Scientific letters of the University of Zilina* **21**(3):77–84, 2019. <https://doi.org/10.26552/com.c.2019.3.77-84>.
- [20] Y. Serhat Erdogan, F. Necati Catbas, P. Gundes Bakir. Structural identification (St-Id) using finite element models for optimum sensor configuration and uncertainty quantification. *Finite Elements in Analysis and Design* **81**:1–13, 2014. <https://doi.org/10.1016/j.finel.2013.10.009>.
- [21] H.-P. Chen, Y.-Q. Ni. *Structural Health Monitoring of Large Civil Engineering Structures*, chap. 5 Modal Analysis of Civil Engineering Structures, pp. 91–121. 2018. <https://doi.org/10.1002/9781119166641.ch5>.
- [22] D. Thorby. *Structural Dynamics and Vibration in Practice*, chap. 13 Vibration of Structures, pp. 367–385. Butterworth-Heinemann, Reading, 2018. <https://doi.org/10.1016/B978-0-7506-8002-8.00013-4>.
- [23] T. Grigorjeva. Numerical analysis of the effects of the bending stiffness of the cable and the mass of structural members on free vibrations of suspension bridges. *Journal of Civil Engineering & Management* **21**(7):948–957, 2015. <https://doi.org/10.3846/13923730.2015.1055787>.
- [24] R. Wendner, A. Strauss, A. Krawtschuk, et al. Assessment of engineering structures based on influence line measurements & model correction approach. In *Proceedings of the 9th International Probabilistic Workshop*. 2011. https://www.researchgate.net/publication/323343059_Assessment_of_Engineering_Structures_based_on_Influence_Line_Measurements_Model_Correction_Approach.
- [25] Google. Bratislava - Raca. [2022-08-02], <https://www.google.sk/maps>.
- [26] V. Dertimanis, E. Chatzi. Sensor networks in structural health monitoring: From theory to practice. *Journal of Sensor and Actuator Networks* **9**(4):47, 2020. <https://doi.org/10.3390/jsan9040047>.
- [27] M. Venglár, K. Lamperová, D. Beutelhauser. *Bridge Safety, Maintenance, Management, Life-Cycle, Resilience and Sustainability*, chap. Application of multipurpose measuring system on various bridges – pros and cons, pp. 324–331. CRC Press, 2022. <https://doi.org/10.1201/9781003322641-36>.
- [28] J. Gocal, L. Ortyl, T. Owerko, et al. *Determination of displacements and vibrations of engineering structures using ground-based radar interferometry*. First printing. Wydawnictwa AGH, Krakow, 2013.
- [29] M. Venglár, M. Sokol. Case study: The Harbor Bridge in Bratislava. *Structural Concrete* **21**(6):2736–2748, 2020. <https://doi.org/10.1002/suco.201900190>.
- [30] J. Krejčí, P. Beneš. A comparison of two modal analysis methods: An impact hammer versus laser vibrometry. *Acta Polytechnica* **60**(5):420–427, 2020. <https://doi.org/10.14311/AP.2020.60.0420>.
- [31] L. Wang, S. Lie, Y. Zhang. Damage detection using frequency shift path. *Mechanical Systems and Signal Processing* **66-67**:298–313, 2016. <https://doi.org/10.1016/j.ymsp.2015.06.028>.
- [32] M. Sokol, M. Venglár. System identification of a composite beam. *Pollack Periodica* **12**(3):43–54, 2017. <https://doi.org/10.1556/606.2017.12.3.5>.
- [33] SÚTN. STN EN 1991-2 Eurocode 1: Actions on structures. Part 2: Traffic loads on bridges, national annex EN 1991-2/NA, 2006.